

Article

Lewis Acid-Induced Change from Four- to Two-Electron Reduction of Dioxygen Catalyzed by Copper Complexes Using Scandium Triflate

Saya Kakuda, Clarence Rolle, Kei Ohkubo, Maxime A. Siegler, Kenneth D. Karlin, and Shunichi Fukuzumi

J. Am. Chem. Soc., **Just Accepted Manuscript** • DOI: 10.1021/ja512584r • Publication Date (Web): 07 Feb 2015

Downloaded from <http://pubs.acs.org> on February 9, 2015

Just Accepted

“Just Accepted” manuscripts have been peer-reviewed and accepted for publication. They are posted online prior to technical editing, formatting for publication and author proofing. The American Chemical Society provides “Just Accepted” as a free service to the research community to expedite the dissemination of scientific material as soon as possible after acceptance. “Just Accepted” manuscripts appear in full in PDF format accompanied by an HTML abstract. “Just Accepted” manuscripts have been fully peer reviewed, but should not be considered the official version of record. They are accessible to all readers and citable by the Digital Object Identifier (DOI®). “Just Accepted” is an optional service offered to authors. Therefore, the “Just Accepted” Web site may not include all articles that will be published in the journal. After a manuscript is technically edited and formatted, it will be removed from the “Just Accepted” Web site and published as an ASAP article. Note that technical editing may introduce minor changes to the manuscript text and/or graphics which could affect content, and all legal disclaimers and ethical guidelines that apply to the journal pertain. ACS cannot be held responsible for errors or consequences arising from the use of information contained in these “Just Accepted” manuscripts.



Lewis Acid-Induced Change from Four- to Two-Electron Reduction of Dioxygen Catalyzed by Copper Complexes Using Scandium Triflate

Saya Kakuda,^{†,*} Clarence Rolle,^{†,*} Kei Ohkubo,[†] Maxime A. Siegler,[‡] Kenneth D. Karlin,^{*,‡} and Shunichi Fukuzumi^{*,†}

[†]Department of Material and Life Science, Division of Advanced Science and Biotechnology, Graduate School of Engineering, ALCA (JST), Osaka University, Suita, Osaka 565-0871, Japan

[‡]Department of Chemistry, Johns Hopkins University, Baltimore, MD 21218, USA

*These authors contributed equally to this work

ABSTRACT: Mononuclear copper complexes, [(tmpa)Cu^{II}(CH₃CN)](ClO₄)₂ (**1**, tmpa = tris(2-pyridylmethyl)amine) and [(BzQ)Cu^{II}(H₂O)₂](ClO₄)₂ (**2**, BzQ = bis(2-quinolinylmethyl)benzylamine), act as efficient catalysts for the selective two-electron reduction of O₂ by ferrocene derivatives in the presence of scandium triflate (Sc(OTf)₃), in acetone, whereas **1** catalyzes the four-electron reduction of O₂ by the same reductant in the presence of Brønsted acids such as triflic acid. Following formation of the peroxo-bridged dicopper(II) complex [(tmpa)Cu^{II}(O₂)Cu^{II}(tmpa)]²⁺, the two-electron reduced product of O₂ with Sc³⁺ is observed to be scandium peroxide ([Sc³⁺(O₂²⁻)]⁺). In the presence of three equiv of hexamethylphosphoric triamide (HMPA), [Sc³⁺(O₂²⁻)]⁺ was oxidized by [Fe(bpy)₃]³⁺ (bpy = 2,2'-bipyridine) to the known superoxide species [(HMPA)₃Sc³⁺(O₂⁻)]²⁺ as detected by EPR spectroscopy. A kinetic study revealed that the rate-determining step of the catalytic cycle for the two-electron reduction of O₂ with **1** is electron transfer from Fc* to **1** to give a cuprous complex which is highly reactive toward O₂, whereas the rate-determining step with **2** is changed to the reaction of the cuprous complex with O₂ following electron transfer from ferrocene derivatives to **2**. The explanation for the change in catalytic O₂-reaction stoichiometry from four-electron with Brønsted acids to two-electron reduction in the presence of Sc³⁺ and also for the change in the rate-determining step is clarified based on a kinetics interrogation of the overall catalytic cycle as well as each step of the catalytic cycle with study of the observed effects of Sc³⁺ on copper-oxygen intermediates.

Introduction

Copper proteins play important roles in oxidation of substrates accompanied by two-electron reduction of dioxygen (O₂) to hydrogen peroxide (H₂O₂) or four-electron reduction of O₂ to water (H₂O) depending on the type of enzymes.¹ For example, in the oxidation of their substrates, galactose oxidases² and amine oxidases³ effect the two-electron reduction of O₂ to hydrogen peroxide⁴ whereas multicopper oxidases (MCO's)⁵ and heme-copper oxidases (HCO's)⁶ facilitate the four-electron reduction of O₂ to H₂O. The catalytic four-electron reduction of O₂ with synthetic copper complexes as well as other metal complexes has merited special attention because of not only the mechanistic interest in relation to MCO's but also in development of a fuel cell technology and their application using earth-abundant metals such as iron, cobalt and copper.⁷⁻¹⁵ On the other hand, the catalytic two-electron reduction of O₂ to H₂O₂ has also attracted increasing interest, because H₂O₂ is regarded as a promising candidate as a high-density energy carrier as compared with gaseous hydrogen and also H₂O₂ can be used as a liquied fuel in simple one-compartment fuel cells.¹⁶⁻¹⁸ There have been many reports on the electrocatalytic and homogeneous four-electron reduction of O₂ with copper complexes.¹⁶⁻²⁴ In contrast, there has been only few examples for the catalytic two-electron reduction of O₂ using a copper complex.²⁵ Whether copper complexes are effective for two-or four-electron reduction of O₂ depends on a

variety of factors, including the ligand type and resulting nature of copper-oxygen intermediates formed as reactive species in the O₂ reduction catalysis.^{24,25} The counter anions of proton sources employed also affects the O₂-reduction catalytic reactivity with copper complexes, with-respect-to the observed stoichiometry and/or mechanism of reaction.^{26,27} However, there has been no report on the change in the number of electrons to reduce O₂ (two-electron vs four-electron) in O₂ reduction catalysis induced by metal ions acting as Lewis acids.

We report herein the drastic change to a two-electron from a four-electron reduction of O₂ with [(tmpa)Cu^{II}(CH₃CN)](ClO₄)₂ (**1**) induced by the Lewis acid [Sc(OTf)₃]. In contrast to the case of **1**, the selective two-electron reduction of O₂ occurred with [(BzQ)Cu^{II}(H₂O)₂](ClO₄)₂ (**2**) in the presence of triflic acid (HOTf) as well as Sc(OTf)₃. The mechanism of the selective two-electron reduction of O₂ with **1** and **2** is examined by a kinetics study of the overall catalytic cycle as well as each step of the catalytic cycle with study of the observed effects of Sc³⁺ on copper-oxygen intermediates.

Experimental Section

Materials. The following reagents were obtained commercially and used as received: Scandium triflate [Sc(OTf)₃], decamethylferrocene (Fc*), 1,1'-dimethylferrocene (Me₂Fc), ferrocene (Fc), perchloric acid (70%), trifluoroacetic acid, hydrogen

peroxide (30%) and NaI (Wako Pure Chemical Industries). Following literature procedures,²⁸ acetone was dried and distilled under Ar. The compounds [(tmpa)Cu^{II}(CH₃CN)](ClO₄)₂ (**1**)²⁹ and bis(2-quinolinylmethyl)benzylamine (BzQ)³⁰ were prepared as described.

[(BzQ)Cu^{II}(H₂O)₂](ClO₄)₂; (**2**) A 50 mL flask with BzQ (389 mg, 1.0 mmol) and Cu(ClO₄)₂·6H₂O (370 mg, 1.0 mmol), as prepared and 20 mL MeOH was then added; the solution became blue and with stirring over 1 h, it yielded a precipitate consisting of blue microcrystals. The solid product **2** was collected employing a vacuum filtration procedure and then washed with 15 mL MeOH, and dried under vacuum. (599 mg, 0.86 mmol, 86% yield) Anal. Calcd (C₂₈H₂₉Cl₂CuO₁₀N₃): C, 47.14; H, 3.96; N, 6.11. Found: C, 47.15; H, 3.87; N, 6.06. X-ray quality crystals were obtained by allowing pentane to slowly diffuse into a saturated acetone solution of **2**.

Single Crystal X-ray Crystallography. All reflection intensities were measured at 110(2) K using a SuperNova diffractometer (with Atlas detector) and Cu K α radiation ($\lambda = 1.54178 \text{ \AA}$) using the CrysAlisPro program (Version 1.171.36.32 Agilent Technologies, 2013); the latter was also employed to refine cell dimensions and for data reduction. The structure was solved and refined on F^2 using SHELXS-2013 (Sheldrick, 2013). Analytical numeric absorption corrections based on a multifaceted crystal model were applied using CrysAlisPro. The data collection temperature was controlled using a Cryojet (Oxford Instruments) system. Unless otherwise specified, the H atoms were placed at calculated positions using AFIX 23, AFIX 43 or AFIX 137 instructions with isotropic displacement parameters with values 1.2 or 1.5 times U_{eq} those for the C atoms attached. The H atoms attached to O1Wn, O2Wn and O3Wn ($n = 1, 2$) (coordinated water molecules) were found from difference Fourier maps, and their coordinates were refined freely (DFIX instructions were used to restrain the O–H and H...H distances within acceptable ranges).

There are three crystallography independent Cu(II) complexes, six ClO₄⁻ perchlorate anions, plus seven lattice acetone solvate molecules per asymmetric unit. The structure is mostly ordered. Five of the six counterions are disordered over two orientations. The occupancy factors of the major components of the disorder refine to 0.871(6), 0.54(2), 0.661(6), 0.591(4), 0.560(16).

C₁₀₂H₁₂₃Cl₆Cu₃N₉O₃₇: moiety formula: 3(C₂₇H₂₇CuN₃O₂), 6(ClO₄), 7(C₃H₆O), Fw = 2470.41, blue block, 0.34 × 0.33 × 0.18 mm³, monoclinic, $P2_1/n$ (no. 14), $a = 22.8236(3)$, $b = 12.18146(19)$, $c = 39.6106(6) \text{ \AA}$, $\beta = 92.6704(13)^\circ$, $V = 11000.8(3) \text{ \AA}^3$, $Z = 4$, $D_x = 1.492 \text{ g cm}^{-3}$, $\mu = 2.760 \text{ mm}^{-1}$, T_{min} – T_{max} : 0.474–0.684. 73408 Reflections were measured up to a resolution of $(\sin \theta/\lambda)_{max} = 0.62 \text{ \AA}^{-1}$. 21523 Reflections were unique ($R_{int} = 0.0243$), of which 19284 were observed [$I > 2\sigma(I)$]. 1682 Parameters were refined using 746 restraints. $R1/wR2$ [$I > 2\sigma(I)$]: 0.0341/0.0914. $R1/wR2$ [all refl.]: 0.0388/0.0948. $S = 1.028$. Residual electron density found between -0.55 and 0.66 e \AA^{-3} . The molecular weight is given for the moiety formula.

Reaction Procedure. Spectral changes (Hewlett Packard 8453 photodiode-array spectrophotometer with a quartz cuvette (path length = 10 mm)) at 298 K were observed as a function of varying Sc(OTf)₃ concentrations during the dioxygen catalytic reduction experiments. Employing a microsyring, an acetone solution of Sc(OTf)₃ was added to an O₂-saturated acetone solution containing [(tmpa)Cu^{II}(CH₃CN)](ClO₄)₂ (**1**) (1.0×10^{-5}

M) or [(BzQ)Cu^{II}(H₂O)₂](ClO₄)₂ (**2**) (1.0×10^{-4} M) and Fc* (2.0×10^{-3} M). Fc* and Me₂Fc⁺ concentrations being produced during the reaction were determined from known absorptivity data, $\lambda_{max} = 780 \text{ nm}$ ($\epsilon = 500 \text{ M}^{-1} \text{ cm}^{-1}$ at 298 K and $600 \text{ M}^{-1} \text{ cm}^{-1}$ at 213 K) for Me₂Fc* and $\lambda_{max} = 650 \text{ nm}$, $\epsilon_{max} = 360 \text{ M}^{-1} \text{ cm}^{-1}$ for Me₂Fc*. For Fc* the extinction coefficient was estimated by carrying out a Fc* electron-transfer oxidation using [Ru^{III}(bpy)₃](PF₆)₃. The limiting concentration of O₂ in an acetone solution was prepared by a mixed gas flow of O₂ and N₂, using a gas mixer (Kofloc GB-3C, KOJIMA Instrument Inc.), that able to effect controlled pressure and flow rate mixing of two gases. Hydrogen peroxide determination was carried out by standard iodide titration where the O₂ reduction product solution in acetone was diluted and reacted with NaI in excess. Quantitation of the I₃⁻ formed was then calculated using its visible spectrum ($\lambda_{max} = 361 \text{ nm}$, $\epsilon = 2.5 \times 10^4 \text{ M}^{-1} \text{ cm}^{-1}$).³¹ All low-temperature UV–vis absorption spectra and spectral changes were recorded using a Hewlett Packard 8453A diode array spectrophotometer with attached liquid nitrogen cooled cryostat (Unisoku USP-203-A).

Kinetic Measurements. Fast reaction with short half-lives ($\leq 10 \text{ s}$) at 298 K were performed with a UNISOKU RSP-601 stopped flow spectrophotometer possessing a MOS-type high selective photodiode array and attached Unisoku thermostated cell holder. The kinetics of electron-transfer from Fc* to **1** were analyzed by monitoring absorption band changes due to Fc* formation. Pseudo-first-order conditions were used throughout, with Fc* concentrations kept at more than a 10-fold excess compared to that of **1**.

Electrochemistry. Copper(II) complex cyclic voltammetry using an ALS 630B electrochemical analyzer was utilized for measurements at 1 atm and under nitrogen or argon, both in the presence and absence of Sc(OTf)₃; conditions included use of deaerated acetone solutions with 0.1 M [(*n*-butyl)₄N]PF₆ (TBAPF₆) all at RT. A platinum working electrode (surface area of 0.3 mm²) was employed within a conventional three-electrode cell using a Pt counter electrode. The BAS platinum working electrode was often polished with an alumina suspension (BAS); prior to use this, acetone was used to wash the electrode. The reference electrode used was Ag/AgNO₃ (0.01 M) and to convert potentials to values vs the SCE, 0.29 V was added.³²

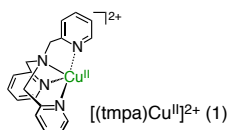
EPR Measurements. A JEOL JES-RE1XE spectrometer was used to record EPR spectra of Cu(II) and scandium superoxide complexes. The modulation amplitude employed was selected to optimize the signal-to-noise (S/N) ratio and resolution under conditions of non-saturating microwave power. A Mn²⁺ marker inserted into the EPR cavity was used to determine g values and hyperfine coupling constants.

Theoretical Calculations. Using a 32-processor Quantum-Cube™ with Gaussian 09 (revision A.02), DFT calculations on copper complexes were performed. A UCAM-B3LYP/6-311G(d) level of theory was employed for geometry optimization.^{33–36} Computational results graphical output were generated using GaussView (ver. 3.09; Semichem, Inc.).³⁷

Results and Discussion

Catalytic Two-Electron Reduction of O₂ by Fc* with **1 in the Presence of Sc(OTf)₃.** We have previously reported that [(tmpa)Cu^{II}(CH₃CN)](ClO₄)₂ (**1**) (tmpa = tris(2-

pyridylmethyl)amine) catalyzed the four-electron reduction of O₂ by decamethylferrocene (Fc^{*}) to H₂O in the presence of perchloric acid or trifluoroacetic acid in acetone as shown in eq 1,



where four-equiv of Fc^{*+} (decamethylferrocinium ion) relative to O₂ were consumed.^{24a,26} When Sc(OTf)₃ is employed as a Lewis acid instead of HClO₄ or CF₃COOH, **1** also efficiently catalyzes the reduction of O₂ where Fc^{*+} is also produced (Figure 1). In this

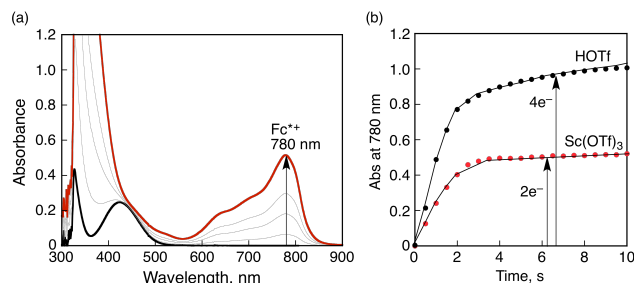
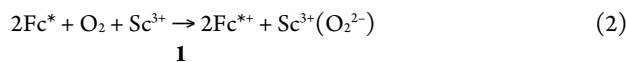


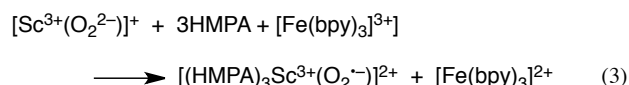
Figure 1. (a) UV-vis spectral changes observed in the two-electron and four-electron reduction of O₂ (0.5 mM) by Fc^{*} (2.0 mM) with Sc(OTf)₃ (2.0 mM) catalyzed by **1** (40 μM) in acetone at 298 K. (b) Time courses of absorbance at 780 nm due to Fc^{*+} in the two-electron and four-electron reduction of O₂ (0.5 mM) by Fc^{*} (2.0 mM) catalyzed by **1** (40 μM) in the presence of Sc(OTf)₃ (2.0 mM) and HOTf (40 mM), respectively.

case, however, the stoichiometry of O₂ reduction is different and follows eq 2,



where two-equivalents of Fc^{*+} (λ_{max} = 780 nm) relative to O₂ are produced and one equiv of Sc³⁺ is consumed instead of four protons (eq 1), as shown in the spectral titration in Figure 2. The reduced product of O₂ is [Sc³⁺(O₂²⁻)]⁺, based on the stoichiometry determined, Figure 2. The yield of [Sc³⁺(O₂²⁻)]⁺ was determined to be 100% based on an iodometric titration (Figure S1 in Supporting Information (SI)).²⁹

To further support the formation of scandium peroxide ([Sc³⁺(O₂²⁻)]⁺), the reaction mixture was oxidized using the one-electron oxidant ([Fe(bpy)₃]³⁺), which was stabilized in the presence of three equiv of the hexamethylphosphoric triamide (HMPA) ligand to produce ([HMPA]₃Sc³⁺(O₂⁻)²⁺), as shown by eq 3.³⁷ The formation of [(HMPA)₃Sc³⁺(O₂⁻)²⁺] was detected



by EPR spectroscopy as shown in Figure 3. The *g* value (2.0112) and superhyperfine coupling constant due to scandium (*I* = 7/2; *a*_{Sc} = 3.82 G) are the same as those reported previously.³⁸ The end-on coordination of O₂⁻ to Sc³⁺ is indicated by inequivalent *a*(¹⁷O) values (14 and 17 G)³⁸ and supported by optimized geometry calculations by an unrestricted Hartree-Fock

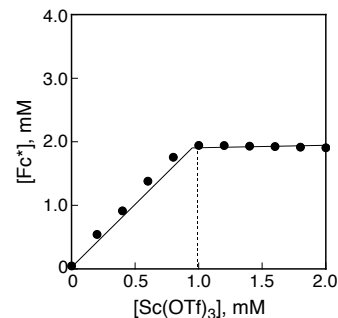


Figure 2. Plot of absorbance at 780 nm due to Fc^{*+} vs concentration of Sc(OTf)₃ in the two-electron reduction of O₂ (2.5 mM) by Fc^{*} (2.0 mM) with Sc(OTf)₃ (0–2.0 mM) catalyzed by **1** (40 μM) in acetone at 298 K.

(UHF) SCF optimization using the 6-311++G** basis set.³⁹ In contrast to the case for this superoxo complex, DFT calculations suggest that the side on structure of the peroxo complex ([Sc³⁺(O₂²⁻)]⁺) is more stable than an end-on coordinated peroxo-scandium species (Figure S2 in SI).

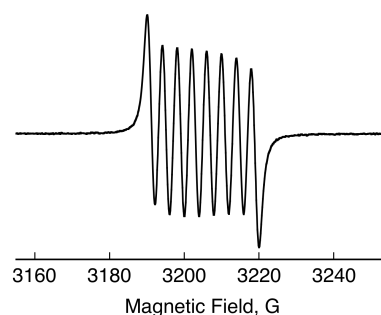


Figure 3. EPR spectrum observed after addition of [Fe^{III}(bpy)₃]³⁺ and HMPA (30 mM) to an N₂-saturated acetone solution of [Sc³⁺(O₂²⁻)]⁺, which was produced by the two-electron reduction of O₂ (11 mM) by Fc^{*} in the presence of [(tmpa)Cu^{II}](ClO₄)₂ (**1**) (10 μM) and Sc(OTf)₃ (10 mM) in acetone at 298 K. The *g* value is 2.011, confirming the production of the known HMPA-Sc-superoxide complex.

Kinetics and Mechanism of Catalytic Two-Electron Reduction of O₂ by Fc^{*} with **1.** The rate of formation of Fc^{*+} in the two-electron reduction of O₂ by Fc^{*} with **1** was monitored by an increase in absorbance at 780 nm due to Fc^{*+}. The rate obeyed pseudo-first-order kinetics in the presence of excess Sc(OTf)₃ and O₂ relative to Fc^{*} (Figure 4a). The observed pseudo-first-order rate constant (*k*_{obs}) increases linearly with increasing concentration of **1** (Figure 4b), whereas the *k*_{obs} value remained constant with increasing concentration of O₂ (Figure 4c). The *k*_{obs} value was also constant at the Sc(OTf)₃ concentration above 5 mM (Figure 4d). Thus, the kinetic formulation of the two-electron reduction of O₂ by Fc^{*} with **1** in the presence of large excess Sc(OTf)₃ is given by eq 4,



where *k*_{cat} is the second-order catalytic rate constant of **1**. The *k*_{cat} value was determined to be (9.4 ± 0.5) × 10⁴ M⁻¹ s⁻¹ at 298 K. This value is twice of the rate constant (*k*_{et}) of electron transfer from Fc^{*} to **1** (5.0 ± 0.1) × 10⁵ M⁻¹ s⁻¹ in acetone at 298 K,^{24a} i.e., *k*_{cat} = 2*k*_{et}, because the electron transfer should occur twice to reduce O₂ in the catalytic cycle when two equiv of Fc⁺ are formed. This indicates that electron transfer from Fc^{*} to **1** is the rate-

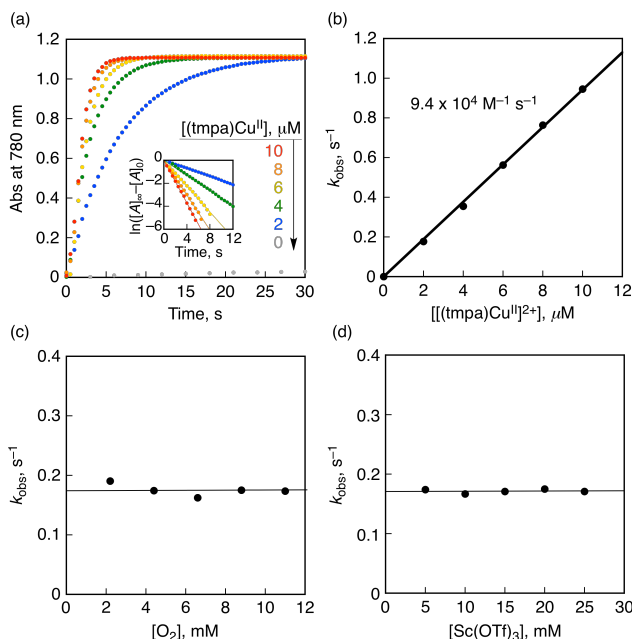


Figure 4. (a) Time profiles of formation of Fc^{2+} monitored by absorbance at 780 nm ($\epsilon = 500 \text{ M}^{-1} \text{ cm}^{-1}$) in the two-electron reduction of O_2 by Fc^* (2.0 mM) with $\text{Sc}(\text{OTf})_3$ (10 mM) catalyzed by **1** (2–10 μM) in saturated ($[\text{O}_2] = 11 \text{ mM}$) acetone at 298 K. Inset: First-order plots. (b) Plot of k_{obs} vs $[\mathbf{1}]$ for the two-electron reduction of O_2 by Fc^* (2.0 mM) in the presence of $\text{Sc}(\text{OTf})_3$ (10 mM) in acetone at 298 K. (c) Plot of k_{obs} vs $[\text{O}_2]$ for the two-electron reduction of O_2 by Fc^* (2.0 mM) catalyzed by **1** (2.0 μM) in saturated ($[\text{O}_2] = 11 \text{ mM}$) acetone at 298 K. (d) Plot of k_{obs} vs $[\text{Sc}(\text{OTf})_3]$ for the two-electron reduction of O_2 by Fc^* (2.0 mM) with $\text{Sc}(\text{OTf})_3$ (5–25 mM) catalyzed by **1** (2 μM) in saturated ($[\text{O}_2] = 11 \text{ mM}$) acetone at 298 K.

determining step in the catalytic two-electron reduction of O_2 by Fc^* with **1**. In such a case, **1** should remain as the cupric complex $[(\text{tmpa})\text{Cu}^{\text{II}}]^{2+}$ during the catalytic two-electron reduction reaction. This was confirmed by the observation of the EPR spectrum of **1** as measured during catalysis as shown in Figure 5, where the EPR spectrum (red line) during the reaction is the same as $[(\text{tmpa})\text{Cu}^{\text{II}}]^{2+}$ before the reaction (black line).

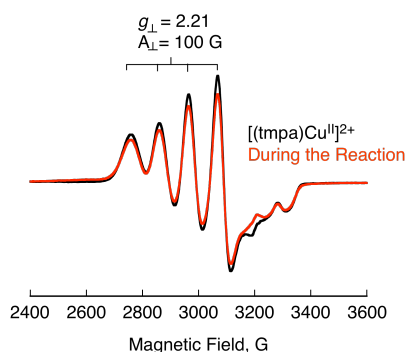


Figure 5. EPR spectra of $[(\text{tmpa})\text{Cu}^{\text{II}}]^{2+}$ **1** (0.10 mM) (black line) measured at 77 K during the catalytic two-electron reduction of O_2 (11 mM) by Fc^* (2 mM) with $\text{Sc}(\text{OTf})_3$ (10 mM) at 298 K (red line). EPR parameters of $[(\text{tmpa})\text{Cu}^{\text{II}}]^{2+}$: $g_{\perp} = 2.21$, $|A_{\perp}| = 100 \text{ G}$, $g_{\parallel} = 2.00$, $|A_{\parallel}| = 64 \text{ G}$.

Electron transfer from Fc^* to **1** is followed by the well-established nearly diffusion controlled binding of O_2 to $[(\text{tmpa})\text{Cu}^{\text{I}}]^{+}$ producing superoxo complex $[(\text{tmpa})\text{Cu}^{\text{I}}(\text{O}_2)]^{+}$ that further rapidly reacts with $[(\text{tmpa})\text{Cu}^{\text{I}}]^{+}$ to afford the peroxo complex (*trans-μ-1,2*-peroxo-dicopper complex

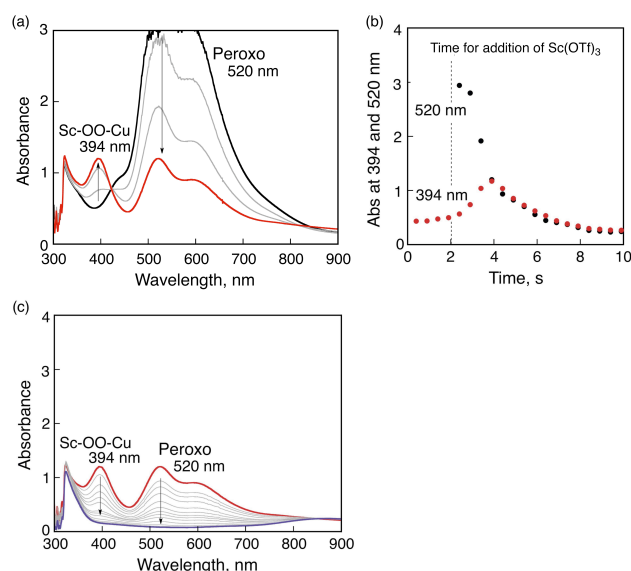


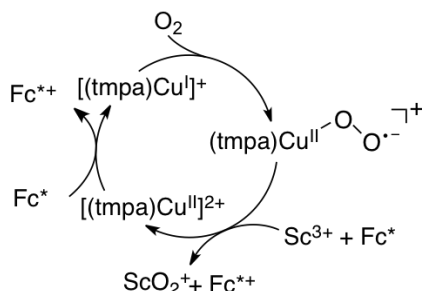
Figure 6. (a,c) UV-vis absorption spectral change in the reaction of $[(\text{tmpa})\text{Cu}^{\text{I}}]^{+}$ (2.0 mM) with O_2 in O_2 -saturated acetone (black), followed by addition of $\text{Sc}(\text{OTf})_3$ (2.0 mM) to the resulting solution at 213 K (red) at (a) 0–4 s and (c) 4–10 s time delays. (b) Absorption time profiles at 394 nm due to the Sc^{3+} -bound peroxo complex, $[(\text{tmpa})\text{Cu}^{\text{I}}(\text{O}_2)\text{Sc}(\text{OTf})_3]^{2+}$ and 520 nm due to $[(\text{tmpa})\text{Cu}^{\text{II}}(\text{O}_2)\text{Cu}^{\text{II}}(\text{tmpa})]^{2+}$. $\text{Sc}(\text{OTf})_3$ was added at 2 s time delay.

$[(\text{tmpa})\text{Cu}^{\text{II}}(\text{O}_2)\text{Cu}^{\text{II}}(\text{tmpa})]^{2+}$) (Figure 6), where the absorption band at 520 nm due to the peroxo complex was observed by the reaction of $[(\text{tmpa})\text{Cu}^{\text{I}}]^{+}$ with O_2 at 213 K.^{24a,26} The addition of one equiv of $\text{Sc}(\text{OTf})_3$ (2 mM) to an acetone solution of the peroxo complex resulted in disappearance of the absorption band due to the peroxo complex, accompanied by appearance of the absorption band at 394 nm, which is tentatively assigned to the Sc^{3+} -bound peroxo complex, $[(\text{tmpa})\text{Cu}^{\text{I}}(\text{O}_2)\text{Sc}(\text{OTf})_3]^{2+}$; the conversion exhibits an isosbestic point (Figures 6a and 6b). At prolonged reaction times, absorption bands at both 394 and 520 nm decayed to yield $[(\text{tmpa})\text{Cu}^{\text{II}}]^{2+}$ (blue line in Figure 6c) and $[\text{Sc}^{3+}(\text{O}_2^{2-})]^{+}$.

Based on the results described above, the catalytic cycle of the two-electron reduction of O_2 by Fc^* with **1** in the presence of $\text{Sc}(\text{OTf})_3$ is proposed as shown in Scheme 1. Electron transfer from Fc^* to **1** is the rate-determining step to produce Fc^{2+} and $[(\text{tmpa})\text{Cu}^{\text{I}}]^{+}$, which rapidly reacts with O_2 to produce the superoxo complex $[(\text{tmpa})\text{Cu}^{\text{I}}(\text{O}_2)]^{+}$. There are two pathways of the further reaction of $[(\text{tmpa})\text{Cu}^{\text{I}}(\text{O}_2)]^{+}$. One is the reaction of $[(\text{tmpa})\text{Cu}^{\text{I}}(\text{O}_2)]^{+}$ with $[(\text{tmpa})\text{Cu}^{\text{I}}]^{+}$ to produce the peroxo complex $[(\text{tmpa})\text{Cu}^{\text{II}}(\text{O}_2)\text{Cu}^{\text{II}}(\text{tmpa})]^{2+}$ which reacts with Sc^{3+} to yield $[(\text{tmpa})\text{Cu}^{\text{II}}]^{2+}$ and $[\text{Sc}^{3+}(\text{O}_2^{2-})]^{+}$ (Figure 6). In such a case, the catalytic rate constant would be the same as the rate constant of electron transfer from Fc^* to $[(\text{tmpa})\text{Cu}^{\text{II}}]^{2+}$ ($k_{\text{cat}} = k_{\text{et}}$). Because $k_{\text{cat}} = 2k_{\text{et}}$ (vide supra), the superoxo complex $[(\text{tmpa})\text{Cu}^{\text{I}}(\text{O}_2)]^{+}$ may be rapidly reduced by Fc^* with Sc^{3+} to produce Fc^{2+} and $[\text{Sc}^{3+}(\text{O}_2^{2-})]^{+}$, accompanied by regeneration of $[(\text{tmpa})\text{Cu}^{\text{II}}]^{2+}$ (Scheme 1).

When $\text{Sc}(\text{OTf})_3$ was replaced by trivalent metal triflates such as $\text{Yb}(\text{OTf})_3$, $\text{Y}(\text{OTf})_3$ and $\text{Lu}(\text{OTf})_3$, which are weaker Lewis acid than $\text{Sc}(\text{OTf})_3$,^{38–40} the catalytic reactivity of the two-electron reduction of O_2 by Fc^* with **1** becomes lower than that the case of $\text{Sc}(\text{OTf})_3$ as shown in Figure 7. Di-valent metal triflates such as $\text{Mg}(\text{OTf})_2$ and $\text{Ca}(\text{OTf})_2$, which are still weaker Lewis acid than trivalent metal triflates,^{39–42} exhibited lower reactivity and the

Scheme 1



reaction was stopped before completion (Figure 7). Thus, strong Lewis acidity of metal ions is required for the efficient catalytic two-electron reduction of O₂ by Fc* with **1**.

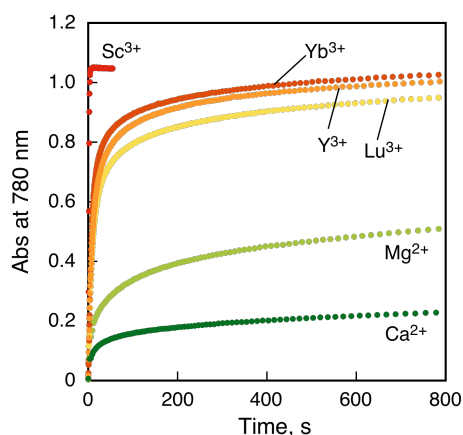


Figure 7. Time courses of absorbance at 780 nm due to Fc*⁺ in the two-electron reduction of O₂ (11 mM) by Fc* (2.0 mM) with metal triflates [Sc(OTf)₃, Yb(OTf)₃, Y(OTf)₃, Lu(OTf)₃, Mg(OTf)₂, and Ca(OTf)₂] (2.0 mM) catalyzed by **1** (40 μM) in acetone at 298 K.

When Fc* was replaced by a weaker one-electron reductant such as 1,1'-dimethylferrocene (Me₂Fc), no electron transfer from Me₂Fc ($E_{\text{ox}} = 0.28$ V vs SCE) to **1** ($E_{\text{red}} = -0.05$ V vs SCE) occurred, leading to no catalytic reduction of O₂ in the presence of Sc(OTf)₃. Thus, we examined the catalytic reduction of O₂ by Me₂Fc in the presence of Sc(OTf)₃ using a copper(II) complex which has a more positive E_{red} value than **1** (vide infra).

Catalytic Two-Electron Reduction of O₂ by Me₂Fc with **2 in the Presence of Sc(OTf)₃.** Pyridyl ligand alterations which introduce steric effects are known to result in a decrease in the donor ability to a Cu(II) center, which causes a positive shift in the redox potential of Cu(II) complexes.²⁹ In order to use milder reductants for the reduction of dioxygen, we synthesized [(BzQ)Cu^{II}](ClO₄)₂ (**2**) as a potential catalyst. Complex **2** was generated by the addition of BzQ to Cu(ClO₄)₂·6H₂O in MeOH and characterized by elemental analysis. Recrystallization of **2** from acetone/pentane afforded crystals suitable for X-ray structure determination; the structure of **2** is shown in Figure 8.⁴³ The steric effect of quinoline ligand is recognized as the elongated Cu-N bonds as compared with those of [(tmpa)Cu^{II}]²⁺.

The E_{red} value of **2** was determined to be 0.44 V vs SCE, which is much more positive than that of **1** (-0.05 V vs SCE), thus the two-electron reduction of O₂ by Me₂Fc became possible using **2** as a catalyst in the presence of Sc(OTf)₃ in acetone at 298 K (eq 5).

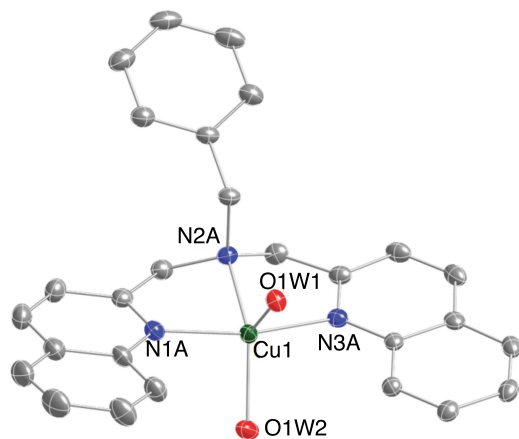
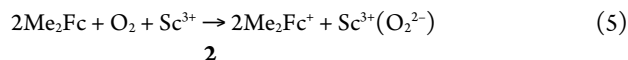


Figure 8. Displacement ellipsoid plot (50% probability level) of one crystallographically independent cation of [Cu^{II}(BzQ)(H₂O)₂](ClO₄)₂·2.33(C₃H₆O) BzQCu^{II}; the two remaining cations, the ClO₄⁻ counteranions, and the lattice acetone solvent molecules have been omitted for clarity. Selected bond distances: Cu1-N1A, 1.9950(14) Å; Cu1-N2A, 2.0494(14) Å; Cu1-N3, 1.9958(14) Å; Cu1-O1W1, 2.1934(12) Å; Cu1-O1W2, 2.0002(13) Å. Selected bond angles: N1A-Cu1-N3A, 165.60(6)°; N1A-Cu1-N2A, 83.21(6)°; N2A-Cu1-N3A, 83.8239(6)°; N1A-Cu1-O1W1, 90.69(5)°; O1W1-Cu1-O1W2, 108.97(5)°; N2A-Cu1-O1W2, 141.95(6)°.

The stoichiometry is the same as in eq 2, where one equiv of Sc³⁺ was consumed for formation of two equiv of Me₂Fc⁺ (Figure S3). Ferrocene itself can also be used to reduce O₂ to [Sc³⁺(O₂²⁻)]⁺ with **2** and Sc(OTf)₃ although the rate is slower than that of Me₂Fc because of the higher E_{ox} value of Fc (0.37 V vs SCE) than that of Me₂Fc ($E_{\text{ox}} = 0.28$ V vs SCE).

The rate of formation of Me₂Fc⁺ obeyed pseudo-zero-order kinetics as shown in Figure 9a, where the initial rate of formation of Me₂Fc⁺ (R_i) is independent of concentration of Me₂Fc. R_i is also independent of concentration of Sc³⁺ (Figure 9b), whereas R_i is proportional to concentrations of O₂ and **2** as shown in Figure 9c and 9d, respectively. Thus, the rate of formation of the two-electron reduction of O₂ by Me₂Fc with **2** in the presence of large excess Sc(OTf)₃ is given by eq 6,

$$d[\text{Me}_2\text{Fc}^+]/dt = k'_{\text{cat}}[\text{O}_2][\mathbf{2}] \quad (6)$$

where k'_{cat} is the second-order catalytic rate constant.

Because the catalytic rate is proportional to concentrations of O₂ and **2**, but independent of concentrations of Me₂Fc or Sc³⁺, the rate-determining step in the catalytic cycle is the reaction of [(BzQ)Cu^I]⁺ with O₂. In such a case, **2** is converted to [(BzQ)Cu^I]⁺ during the catalytic two-electron reduction of O₂ by Me₂Fc with **2**. This was confirmed by disappearance of the EPR spectrum of **2** measured during the catalysis as shown in Figure 10, where the EPR signal due to **2** (black line) is converted to the Cu^I complex, which is EPR silent (red line).

The reaction of the Cu^I complex of **2** with O₂ was previously reported to afford copper(II)-oxygen intermediates different than that known for the case of **1**, that are a (η^2 : η^2 -peroxo)dicopper(II) complex ($\lambda_{\text{max}} = 362$ and 535 nm) plus a

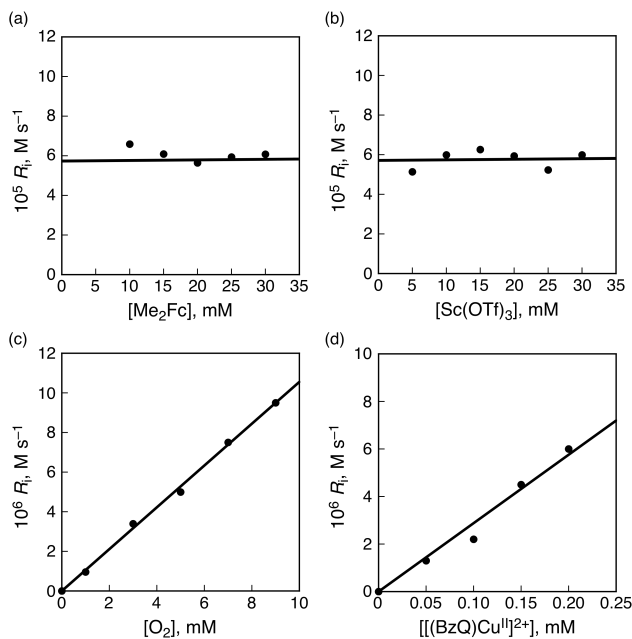


Figure 9. (a) Plot of the initial rate of formation of Me_2Fc^+ vs $[\text{Me}_2\text{Fc}]$ in the two-electron reduction of O_2 by Me_2Fc with $\text{Sc}(\text{OTf})_3$ (10 mM) catalyzed by **2** (0.2 mM) in saturated ($[\text{O}_2] = 11$ mM) acetone at 298 K. (b) Plot of the initial rate of formation of Me_2Fc^+ vs $[\text{Sc}(\text{OTf})_3]$ in the two-electron reduction of O_2 by Me_2Fc (10 mM) with $\text{Sc}(\text{OTf})_3$ catalyzed by **2** (0.20 mM) in saturated ($[\text{O}_2] = 11$ mM) acetone at 298 K. (c) Plot of k_{obs} vs $[\text{O}_2]$ for the two-electron reduction of O_2 by Me_2Fc (10 mM) with $\text{Sc}(\text{OTf})_3$ (10 mM) catalyzed by **2** (0.2 mM) in acetone at 298 K. (d) Plot of k_{obs} vs $[\text{2}]$ for the two-electron reduction of O_2 by Me_2Fc (10 mM) with $\text{Sc}(\text{OTf})_3$ (10 mM) catalyzed by **2** in saturated ($[\text{O}_2] = 11$ mM) acetone at 298 K.

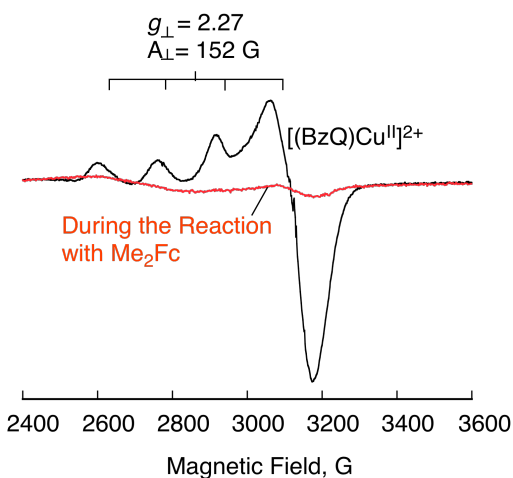


Figure 10. EPR spectra of $[(\text{BzQ})\text{Cu}^{\text{II}}]^{2+}$ (**2**) (0.10 mM) (black line) observed at 77 K, $[(\text{BzQ})\text{Cu}^{\text{I}}]^+$ (0.05 mM) produced during the catalytic reduction of oxygen (2.2 mM) in the presence of Me_2Fc (10 mM) and $\text{Sc}(\text{OTf})_3$ (10 mM) (red line).

bis(μ -oxo)dicopper(III) species ($\lambda_{\text{max}} = 394$ nm) (see Figure 11a, black line); the mixture had been characterized by resonance Raman spectroscopy.²⁹ The addition of 2 equiv HOTf to an acetone solution of the peroxo and bis- μ -oxo complexes resulted in the decomposition of the Cu-O_2 species to release H_2O_2 (Figure 11b). In contrast, the addition of $\text{Sc}(\text{OTf})_3$ to an acetone solution of the peroxo and bis- μ -oxo complexes resulted in little change in absorption bands of the Cu-O_2 intermediates (Figure 11c), indicating that these complexes are stable against Sc^{3+} (Scheme 2).

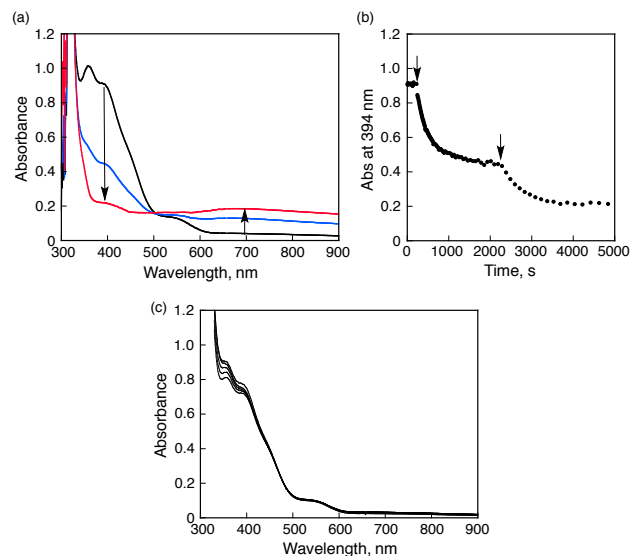
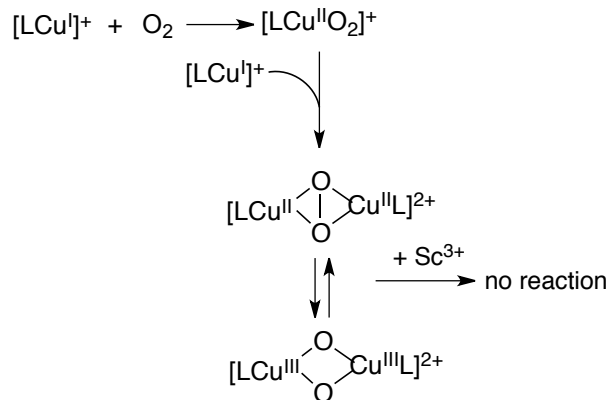


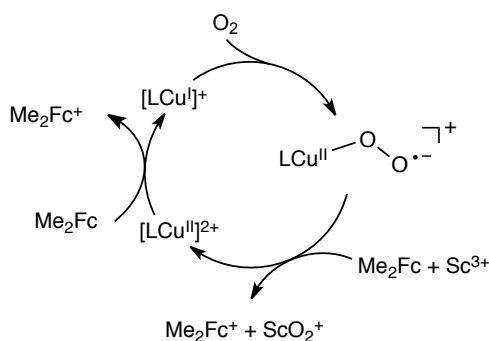
Figure 11. (a) UV-vis spectral changes observed upon the addition of 2 eq of HOTf (4.0 mM) to the mixture of the μ - η^2 - η^2 -(side-on) peroxo dinuclear copper(II) complex and the bis- μ -oxo dinuclear copper(III) complex. (b) Absorption time profiles at 394 nm due to the addition of HOTf (4.0 mM) to the mixture of the μ - η^2 - η^2 -(side-on) peroxo dinuclear copper(II) complex and the bis- μ -oxo dinuclear copper(III) complex. (c) UV-vis spectral changes observed upon the addition of $\text{Sc}(\text{OTf})_3$ (4.0 mM) to the mixture of the μ - η^2 - η^2 -(side-on) peroxo dinuclear copper(II) complex and the bis- μ -oxo dinuclear copper(III) complex.

Scheme 2



Thus, once the μ - η^2 - η^2 -(side-on) peroxo dinuclear copper(II) complex and the bis- μ -oxo dinuclear copper(III) complex are formed via the superoxo complex, no catalytic reduction of O_2 by Me_2Fc would occur with **2** in the presence of $\text{Sc}(\text{OTf})_3$. Under the catalytic conditions, the superoxo complex is reduced by Me_2Fc in the presence of Sc^{3+} to yield Me_2Fc^+ and $\text{Sc}(\text{O}_2)^+$, accompanied by regeneration of **2** without formation of the μ - η^2 - η^2 -(side-on) peroxo dinuclear copper(II) complex or the bis- μ -oxo dinuclear copper(III) complex as shown in Scheme 3. The rate-determining step in Scheme 3 is the reaction of $[(\text{BzQ})\text{Cu}^{\text{I}}]^+$ with O_2 to produce the superoxo complex, when the catalytic rate is proportional to concentrations of O_2 and **2**, but independent of concentrations of Me_2Fc or Sc^{3+} as observed in Figure 9.

Scheme 3



Conclusion

The four-electron reduction of O_2 by Fc^* with a mononuclear complex $[(tmpa)Cu^{II}](ClO_4)_2$ (**1**) in the presence of a proton source (HOTf) was changed to the two-electron reduction of O_2 by replacing Brønsted acids by $Sc(OTf)_3$ that acts as a strong Lewis acid. The rate-determining step of the catalytic cycle is found to be electron transfer from Fc^* to O_2 . When **1** was replaced by a copper(II) complex $[(BzQ)Cu^{II}](ClO_4)_2$ (**2**), which has a more positive reduction potential as compared with **1**, the catalytic two-electron reduction of O_2 is made possible by using a weaker one-electron reductant than Fc^* such as Me_2Fc and Fc . In this case, the rate-determining step is the reaction of $[(BzQ)Cu^{II}]^+$ with O_2 to produce the superoxo complex. The Lewis acid-induced change in the stoichiometry of the catalytic O_2 reduction provides a new way to control this important biological or chemical “fuel-cell” reaction which can produce either hydrogen peroxide or water.

ASSOCIATED CONTENT

Supporting Information. Spectral and kinetic analytical data, theoretical calculation data (Figures S1-S6), and X-ray crystallographic data (pdf); crystallographic file (cif). This material is available free of charge via the Internet at <http://pubs.acs.org>.

AUTHOR INFORMATION

Corresponding Author

fukuzumi@chem.eng.osaka-u.ac.jp; karlin@jhu.edu

ACKNOWLEDGMENT

This work was supported by an Advanced Low Carbon Technology Research and Development (ALCA) program from Japan Science Technology Agency (JST) to S.F., the Japan Society for the Promotion of Science (JSPS: Grants 20108010 to S.F. and 26620154 and 26288037 to K.O.) sponsored by the MEXT (Japan), and by KOSEF/MEST through the WCU Project (R31-2008-000-10010-0). K.D.K. also acknowledges support from the USA National Institutes of Health.

REFERENCES

- (1) (a) Solomon, E. I.; Heppner, D. E.; Johnston, E. M.; Ginsbach, J. W.; Cirera, J.; Qayyum, M.; Kieber-Emmons, M. T.; Kjaergaard, C. H.; Hadt, R. G.; Tian, L. *Chem. Rev.* **2014**, *114*, 3659. (b) Kosman, D. J. *J. Biol. Inorg. Chem.* **2010**, *15*, 15. (c) Battaini, G.; Granata, A.; Monzani, E.; Gullotti, M.; Casella, L. *Adv. Inorg. Chem.* **2006**, *58*, 185. (d) Rosenzweig, A. C. *Nat. Chem.* **2009**, *1*, 684.
- (2) Humphreys, K. J.; Mirica, L. M.; Wang, Y.; Klinman, J. P. *J. Am. Chem. Soc.* **2009**, *131*, 4657–4663.

- (3) Mukherjee, A.; Smirnov, V. V.; Lanci, M. P.; Brown, D. E.; Shepard, E. M.; Dooley, D. M.; Roth, J. P. *J. Am. Chem. Soc.* **2008**, *130*, 9459–9473.
- (4) McGuirl, M. A.; Dooley, D. M. Copper Proteins with Type 2 Sites. In *Encyclopedia of Inorganic Chemistry*, 2nd ed.; King, R. B., Ed.; John Wiley & Sons Ltd.: Chichester, 2005; Vol. II, pp 1201–1225.
- (5) (a) Blanford, C. F.; Heath, R. S.; Armstrong, F. A. *Chem. Commun.* **2007**, 1710. (b) Mano, N.; Soukharev, V.; Heller, A. *J. Phys. Chem. B* **2006**, *110*, 11180–11187.
- (6) (a) Pereira, M. M.; Santana, M.; Teixeira, M. *Biochim. Biophys. Acta* **2001**, *1505*, 185. (b) Winter, M.; Brodd, R. J. *Chem. Rev.* **2004**, *104*, 4245. (c) Ferguson-Miller, S.; Babcock, G. T. *Chem. Rev.* **1996**, *96*, 2889. (d) Hosler, J. P.; Ferguson-Miller, S.; Mills, D. A. *Annu. Rev. Biochem.* **2006**, *75*, 165. (e) Kaila, V. R. I.; Verkhovsky, M. I.; Wikström, M. *Chem. Rev.* **2010**, *110*, 7062.
- (7) (a) Fukuzumi, S.; Karlin, K. D. *Coord. Chem. Rev.* **2013**, *257*, 187. (b) Fukuzumi, S. *Chem. Lett.* **2008**, *37*, 808.
- (8) (a) Collman, J. P.; Devaraj, N. K.; Decréau, R. A.; Yang, Y.; Yan, Y.-L.; Ebina, W.; Eberspacher, T. A.; Chidsey, C. E. D. *Science* **2007**, *315*, 1565. (b) Collman, J. P.; Decréau, R. A.; Lin, H.; Hosseini, A.; Yang, Y.; Dey, A.; Eberspacher, T. A. *Proc. Natl. Acad. Sci. U.S.A.* **2009**, *106*, 7320. (c) Collman, J. P.; Ghosh, S.; Dey, A.; Decréau, R. A.; Yang, Y. *J. Am. Chem. Soc.* **2009**, *131*, 5034.
- (9) (a) Rosenthal, J.; Nocera, D. G. *Acc. Chem. Res.* **2007**, *40*, 543. (b) Chang, C. J.; Loh, Z.-H.; Shi, C.; Anson, F. C.; Nocera, D. G. *J. Am. Chem. Soc.* **2004**, *126*, 10013. (c) Dogutan, D. K.; Stoian, S. A.; McGuire, R.; Schwalbe, M.; Teets, T. S.; Nocera, D. G. *J. Am. Chem. Soc.* **2011**, *133*, 131. (d) Teets, T. S.; Cook, T. R.; McCarthy, B. D.; Nocera, D. G. *J. Am. Chem. Soc.* **2011**, *133*, 8114.
- (10) (a) Halime, Z.; Kotani, H.; Li, Y.; Fukuzumi, S.; Karlin, K. D. *Proc. Natl. Acad. Sci. U.S.A.* **2011**, *108*, 13990. (b) Fukuzumi, S.; Okamoto, K.; Gros, C. P.; Guillard, R. J. *Am. Chem. Soc.* **2004**, *126*, 10441. (c) Fukuzumi, S.; Okamoto, K.; Tokuda, Y.; Gros, C. P.; Guillard, R. J. *Am. Chem. Soc.* **2004**, *126*, 17059. (d) Fukuzumi, S.; Mandal, S.; Mase, M.; Ohkubo, K.; Park, H.; Benet-Buchholz, J.; Nam, W.; Llobet, A. *J. Am. Chem. Soc.* **2012**, *134*, 9906.
- (11) (a) Fukuzumi, S.; Mochizuki, S.; Tanaka, T. *Inorg. Chem.* **1989**, *28*, 2459. (b) Fukuzumi, S.; Mochizuki, S.; Tanaka, T. *Inorg. Chem.* **1990**, *29*, 653. (c) Fukuzumi, S.; Mochizuki, S.; Tanaka, T. *J. Chem. Soc., Chem. Commun.* **1989**, 391.
- (12) Vielstich, W.; Lamm, A.; Gasteiger, H. A. *Handbook of fuel cells: fundamentals, technology, and applications*; Wiley: Chichester, U.K.; Hoboken, NJ, 2003.
- (13) (a) Zagal, J. H.; Griveau, S.; Silva, J. F.; Nyokong, T.; Bedioui, F. *Coord. Chem. Rev.* **2010**, *254*, 2755. (b) Li, W.; Yu, A.; Higgins, D. C.; Llanos, B. G.; Chen, Z. *J. Am. Chem. Soc.* **2010**, *132*, 17056.
- (14) (a) Gewirth, A. A.; Thorum, M. S. *Inorg. Chem.* **2010**, *49*, 3557. (b) Stambouli, A. B.; Traversa, E. *Renew. Sust. Energy Rev.* **2002**, *6*, 295. (c) Marković, N. M.; Schmidt, T. J.; Stamenković V.; Ross, P. N. *Fuel Cells* **2001**, *1*, 105. (d) Steele, B. C. H.; Heinzel, A. *Nature* **2001**, *414*, 345.
- (15) Asahi, M.; Yamazaki, S.-i.; Itoh, S.; Ioroi, T. *Dalton Trans.* **2014**, 43, 10705.
- (16) (a) Honda, T.; Kojima, T.; Fukuzumi, S. *J. Am. Chem. Soc.* **2012**, *134*, 4196. (b) Mase, K.; Ohkubo, K.; Fukuzumi, S. *J. Am. Chem. Soc.* **2013**, *135*, 2800.
- (17) (a) Disselkamp, R. S. *Energy Fuels* **2008**, *22*, 2771. (b) Disselkamp, R. S. *Int. J. Hydrogen Energy* **2010**, *35*, 1049.
- (18) (a) Fukuzumi, S.; Yamada, Y.; Karlin, K. D. *Electrochim. Acta* **2012**, *82*, 493. (b) Yamada, Y.; Fukunishi, Y.; Yamazaki, S.; Fukuzumi, S. *Chem. Commun.* **2010**, 46, 7334. (c) Yamada, Y.; Yoshida, S.; Honda, T.; Fukuzumi, S. *Energy Environ. Sci.* **2011**, *4*, 2822. (d) Shaegh, S. A. M.; Nguyen, N.-T.; Ehteshami, S. M. M.; Chan, S. H. *Energy Environ. Sci.* **2012**, *5*, 8225.
- (19) (a) Zhang, J.; Anson, F. C. *J. Electroanal. Chem.* **1992**, *341*, 323. (b) Zhang, J.; Anson, F. C. *J. Electroanal. Chem.* **1993**, *348*, 81. (b) Zhang, J.; Anson, F. C. *Electrochim. Acta* **1993**, *38*, 2423. (c) Lei, Y.; Anson, F. C. *Inorg. Chem.* **1994**, *33*, 5003.

- 1
2
3
4
5
6
7
8
9
10
11
12
13
14
15
16
17
18
19
20
21
22
23
24
25
26
27
28
29
30
31
32
33
34
35
36
37
38
39
40
41
42
43
44
45
46
47
48
49
50
51
52
53
54
55
56
57
58
59
60
- (20) (a) Weng, Y. C.; Fan, F.-R. F.; Bard, A. J. *J. Am. Chem. Soc.* **2005**, *127*, 17576. (b) Thorum, M. S.; Yadav, J.; Gewirth, A. A. *Angew. Chem., Int. Ed.* **2009**, *48*, 165.
- (21) (a) McCrory, C. C. L.; Ottenwaelder, X.; Stack, T. D. P.; Chidsey, C. E. D. *J. Phys. Chem. A* **2007**, *111*, 12641. (b) McCrory, C. C. L.; Devadoss, A.; Ottenwaelder, X.; Lowe, R. D.; Stack, T. D. P.; Chidsey, C. E. D. *J. Am. Chem. Soc.* **2011**, *133*, 3696.
- (22) (a) Pichon, C.; Mialane, P.; Dolbecq, A.; Marrot, J.; Riviere, E.; Keita, B.; Nadjo, L.; Secheresse, F. *Inorg. Chem.* **2007**, *46*, 5292. (b) Dias, V. L. N.; Fernandes, E. N.; da Silva, L. M. S.; Marques, E. P.; Zhang, J.; Marques, A. L. B. *J. Power Sources* **2005**, *142*, 10. (c) Losada, J.; del Peso, L.; Beyer, L. *Inorg. Chim. Acta* **2001**, *321*, 107.
- (23) (a) Thorseth, M. A.; Tornow, C. E.; Tse, E. C. M.; Gewirth, A. A. *Coord. Chem. Rev.* **2013**, *257*, 130. (b) Thorseth, M. A.; Letko, C. S.; Rauchfuss, T. B.; Gewirth, A. A. *Inorg. Chem.* **2011**, *50*, 6158.
- (24) (a) Fukuzumi, S.; Kotani, H.; Lucas, H. R.; Doi, K.; Suenobu, T.; Peterson, R. L.; Karlin, K. D. *J. Am. Chem. Soc.* **2010**, *132*, 6874. (b) Fukuzumi, S.; Tahsini, L.; Lee, Y.-M.; Ohkubo, K.; Nam, W.; Karlin, K. D. *J. Am. Chem. Soc.* **2012**, *134*, 7025. (c) Tahsini, L.; Kotani, H.; Lee, Y.-M.; Cho, J.; Nam, W.; Karlin, K. D.; Fukuzumi, S. *Chem.–Eur. J.* **2012**, *18*, 1084. (d) Das, D.; Lee, Y.-M.; Ohkubo, K.; Nam, W.; Karlin, K. D.; Fukuzumi, S. *J. Am. Chem. Soc.* **2013**, *135*, 4018.
- (25) Das, D.; Lee, Y.-M.; Ohkubo, K.; Nam, W.; Karlin, K. D. Fukuzumi, S. *J. Am. Chem. Soc.* **2013**, *135*, 2825.
- (26) Kakuda, S.; Peterson, R. L.; Ohkubo, K.; Karlin, K. D.; Fukuzumi, S. *J. Am. Chem. Soc.* **2013**, *135*, 2825.
- (27) Armarego, W. L. F.; Chai, C. L. L. *Purification of Laboratory Chemicals*, 5th ed.; Butterworth-Heinemann: Oxford, 2003.
- (28) Wang, J.; Schopfer, M. P.; Puii, S. C.; Sarjeant, A. A. N.; Karlin, K. D. *Inorg. Chem.* **2010**, *49*, 1404.
- (29) Kryatov, S. V.; Taktak, S.; Korendovych, I. V.; Rybak-Akimova, E. V.; Kaizer, J.; Torelli, S.; Shan, X.; Mandal, S.; MacMurdo, V.; Mairata i Payeras, A.; Que, L., Jr. *Inorg. Chem.* **2005**, *44*, 85.
- (30) Kunishita, A.; Osako, T.; Tachi, Y.; Teraoka, J.; Itoh, S. *Bull. Chem. Soc. Jpn.* **2006**, *79*, 1729.
- (31) (a) Mair, R. D.; Graupner, A. J. *J. Anal. Chem.* **1964**, *36*, 194. (b) Fukuzumi, S.; Kuroda, S.; Tanaka, T. *J. Am. Chem. Soc.* **1985**, *107*, 3020.
- (32) Mann, C. K.; Barnes, K. K. *Electrochemical Reactions in Nonaqueous Systems*; Marel Dekker; New York, 1990.
- (33) (a) Becke, A. D. *J. Chem. Phys.* **1993**, *98*, 5648. (b) Lee, C.; Yang W.; Parr, R. G. *Phys. Rev. B* **1988**, *37*, 785.
- (34) (a) Hay, P. J.; Wadt, W. R. *J. Chem. Phys.* **1985**, *82*, 270. (b) Curtiss, L. A.; McGrath, M. P.; Blauddau, J.-P.; Davis, N. E.; Binning, R. C. Jr.; Radom, L. *J. Chem. Phys.* **1995**, *103*, 6104.
- (35) (a) Yanai, T.; Tew, D. P.; Handy, N. C. *Chem. Phys. Lett.* **2004**, *393*, 51. (b) Tawada, Y.; Tsuneda, T.; Yanagisawa, S.; Yanai, T.; Hirao, K. *J. Chem. Phys.* **2004**, *120*, 8425.
- (36) Takaichi, J.; Ohkubo, K.; Sugimoto, H.; Nakano, M.; Usa, D.; Maekawa, H.; Fujieda, N.; Nishiwaki, N.; Seki, S.; Fukuzumi, S.; Itoh, S. *Dalton Trans.* **2013**, *42*, 2438.
- (37) Dennington, R., II; Keith, T.; Millam, J.; Eppinnett, K.; Hovell, W. L.; Gilliland, R. *Gaussview*; Semichem, Inc.: Shawnee Mission, KS, 2003.
- (38) (a) Fukuzumi, S.; Patz, M.; Suenobu, T.; Kuwahara, Y.; Itoh, S. *J. Am. Chem. Soc.* **1999**, *121*, 1605. (b) Kawashima, T.; Ohkubo, K.; Fukuzumi, S. *Phys. Chem. Chem. Phys.* **2011**, *13*, 3344.
- (39) (a) Fukuzumi, S.; Ohkubo, K. *Chem.–Eur. J.* **2000**, *6*, 4532. (b) Fukuzumi, S.; Ohkubo, K. *J. Am. Chem. Soc.* **2002**, *124*, 10270.
- (40) Fukuzumi, S. *Prog. Inorg. Chem.* **2009**, *56*, 49. (b) Fukuzumi, S.; Ohkubo, K.; Morimoto, Y. *Phys. Chem. Chem. Phys.* **2012**, *14*, 8472.
- (41) Morimoto, Y.; Kotani, H.; Park, J.; Lee, Y.-M.; Nam, W.; Fukuzumi, S. *J. Am. Chem. Soc.* **2011**, *133*, 403.
- (42) When a weak Lewis acid, Mg(OTf)₂ was applied to the catalyst for the O₂ reduction reaction with Fc*, the absorption changes for formation of Fc** were significantly smaller as compared with the case of Sc(OTf)₃, as shown in Figure 7.
- (43) The crystal structure of a similar copper(II) complex of BzQ type ligand have already been reported. Osako, T.; Nagatomo, S.; Kitagawa, T.; Cramer, C. J.; Itoh, S. *J. Biol. Inorg. Chem.* **2005**, *10*, 581.

TOC Graphic

